

# Multiwalled Carbon Nanotube Filters for Toxin Removal from Cigarette Smoke

Sumit Kumar Pandey, Pramod Kumar Vishwakarma, Sunil Kumar Yadav, Prashant Shukla, and Anchal Srivastava\*

**Cite This:** *ACS Appl. Nano Mater.* 2020, 3, 760–771

**Read Online**

ACCESS |

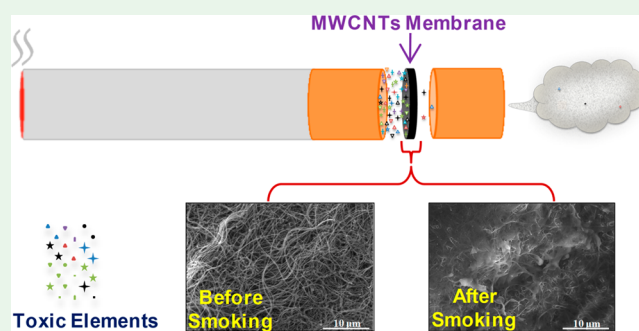
Metrics & More

Article Recommendations

Supporting Information

**ABSTRACT:** The fatal diseases and disorders caused by smoking have raised a serious concern for worldwide public health. So for its prevention, it has become very necessary to develop various types of filter material for the removal of carcinogenic and other toxic elements present in cigarette smoke. Herein, we demonstrate a novel filter for cigarettes, fabricated by the insertion of multiwalled carbon nanotubes (MWCNTs) based thin flexible membrane into the conventional cellulose acetate filter. The developed filter has attractive attributes of high filtering efficiency, lightweight, flexible, cost-effective, and scalable production. This flexible MWCNTs membrane has been fabricated using a simple vacuum-assisted filtration technique followed by the synthesis of MWCNTs using a cost-effective spray pyrolysis technique. The filter shows excellent performance for the removal of  $PM_{2.5}$ , having a removal efficiency of ~99%. It also shows a significant ability to remove nicotine, tar, and toxic heavy metals such as lead present in cigarette smoke.

**KEYWORDS:** MWCNTs membrane, particulate matter, heavy metals, nicotine, tar



## 1. INTRODUCTION

Cigarette smoking is one of the biggest threats that has ever been faced by worldwide public health.<sup>1</sup> It causes more than 7 million deaths every year, which is more than the total deaths caused by human immunodeficiency virus/acquired immunodeficiency syndrome (HIV/AIDS), tuberculosis, and malaria.<sup>2</sup> More than 6 million deaths are the result of direct smoking, while about 890,000 deaths are the result of passive smoking. Further, recent studies show that, if effective measures are not taken immediately, this epidemic can cause more than 1 billion deaths in the 21st century.<sup>2,3</sup> Several attempts have been made to reduce the epidemic caused by smoking, but the desired success has not been achieved so far. Therefore, to reduce the effect of this epidemic, the elimination of carcinogenic and other harmful chemicals/compounds present in the cigarette smoke is highly desired.

Cigarette smoke is an aerosol containing more than thousands of chemical compounds including nicotine, tar, particulate matters (PM), heavy metals (arsenic, chromium, cadmium, lead, etc.), polycyclic aromatic hydrocarbons, etc. with its many carcinogens and other harmful constituents, which are present in both the particulate and vapor phases.<sup>4</sup> Breathing in this toxic smoke of cigarette is a major factor for many types of carcinogenic and deadly diseases such as cancer, asthma, hypertension, etc.<sup>5–14</sup>

The particulate matters (PM) present in smoke is a complex mixture of tiny particles and liquid droplets composed of various organic and inorganic chemical compounds such as elemental carbon, silicates, sulfates, nitrates etc.,<sup>15–17</sup> which is a serious health hazard for smokers as well as for the passive smokers. On the basis of particle size, PM has been classified into three categories: (i) coarse particles having a diameter between 10 to 2.5  $\mu\text{m}$  known as  $PM_{10}$ , (ii) fine particles having a diameter between 2.5 to 0.1  $\mu\text{m}$  known as  $PM_{2.5}$ , and (iii) ultra-fine particles having diameter less than 0.1  $\mu\text{m}$  known as  $PM_{0.1}$ .<sup>18</sup> Among these,  $PM_{2.5}$  is a serious threat to human health since it carries many toxic chemicals/compounds that can penetrate the human bronchi and lungs due to its small size.<sup>19</sup> Therefore, long-term intake of  $PM_{2.5}$  increases morbidity and mortality.<sup>20–22</sup> In the same way, the heavy metals present in cigarette smoke such as nickel, cobalt, copper, zinc, lead, cadmium, etc. are also widely known for their toxic nature, which adversely affects human health.<sup>23–26</sup> These heavy metals also accumulate in tissues and fluids through smoking and lead to a cancer risk.<sup>27–29</sup> Therefore, they have

**Received:** November 19, 2019

**Accepted:** December 26, 2019

**Published:** December 26, 2019

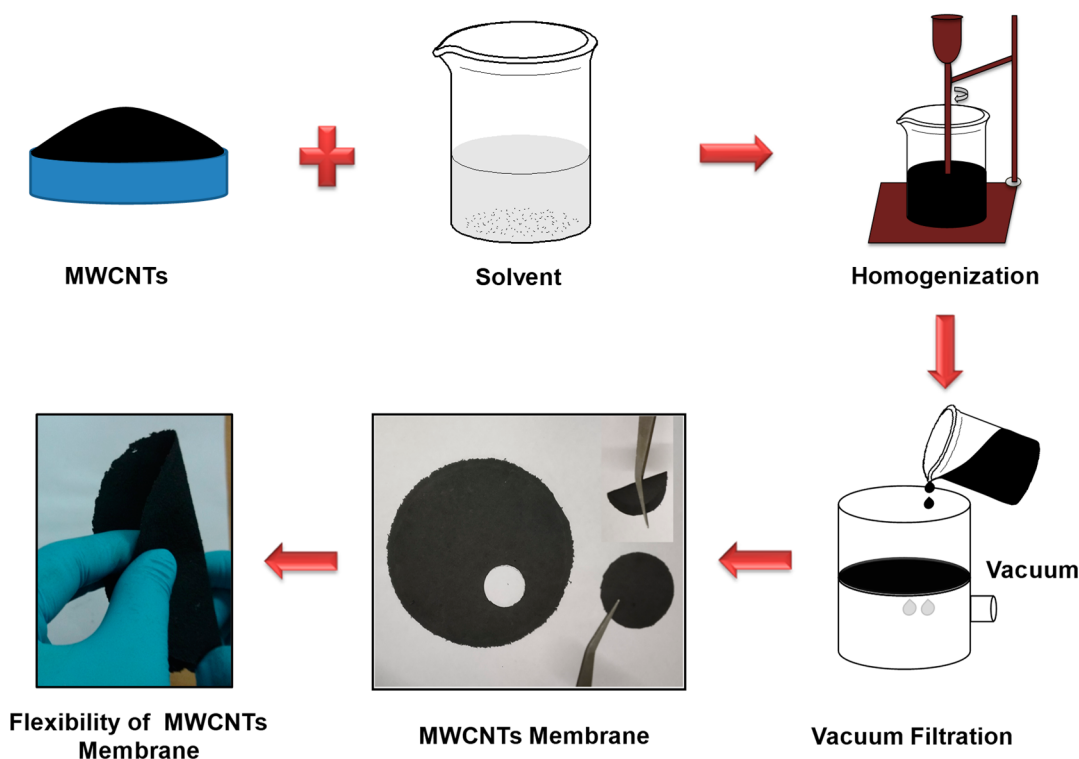


**Figure 1.** Schematic of fabrication process for the preparation of flexible MWCNTs membrane using vacuum-assisted filtration technique.

also been paid much more attention due to their direct relation with the smoker's health.

Nicotine, which is one of the main constituents of cigarette smoke, has serious side effects in addition to being highly addictive. An average cigarette contains about 2 mg of absorbed nicotine, which is too much for an unrestricted smoker.<sup>30</sup> Its excessive intake adversely affects the heart, lung, kidney, reproductive systems, etc. of the smoker.<sup>31</sup> Therefore, for its balanced and safe intake, it is of utmost important to reduce its concentration from cigarette smoke.

In view of the above-discussed adverse effects of these toxic constituents, it has become a great desire to remove them from cigarette smoke. In this respect, a series of nanostructured adsorbing materials have been considered for the removal of toxic chemicals/compounds from cigarette smoke.<sup>29,32–39</sup> For example, Guangda et al.<sup>34</sup> have reported the removal of 75.95% of phenolic compounds, 55.00% of ammonia, and 56.80% of particulate matter from cigarette smoke using carbon nanocages. In another work, Zhou et al.<sup>33</sup> have reported the removal of toxic heavy metals such as 16% nickel, 50% chromium, 45% lead, and 55% cadmium from cigarette smoke using chitosan. In another work, Hubetska et al.<sup>40</sup> have reported a comparative estimation of the extraction efficiency of nicotine by a commercial activated charcoal and a synthesized ordered spherical mesoporous charcoal adsorbent. In these reports, authors have used nanostructured adsorbents to filter the toxins from cigarette smoke, which generally removes the toxic constituents from cigarette smoke through a physisorption process. In this process, surface area, porosity, geometrical structure, moisture resisting capability, etc. play an important role. Along with these properties, the forms of nanostructured adsorbents are also very important. In the above reports, authors have used the powder form of these nanostructured adsorbents, which possesses many disadvantages such as the granular size of such a type of materials are

not fixed, therefore rendering the filter rod is more difficult. As a result, sometimes polymers or binders have been used to hold them together, but the use of these additive materials reduces the adsorption efficiency as well as affects the taste of the smoke. These additive materials also react with smoke constituents and form poisonous compounds.<sup>41–43</sup> The above materials and methods are very tedious and expensive too. Therefore, we need to explore other effective materials with a superior adsorption property to enhance the removal efficiency of toxic compounds from cigarette smoke. Moreover, some theoretical investigations have also been reported for the removal of toxins from cigarette smoke. For example, Yoosefian et al.<sup>44</sup> have reported the removal of the acrolein carcinogen from cigarette smoke using carboxylated single walled carbon nanotubes as a general nanofilter platform. In another report Yoosefian<sup>45</sup> has reported the removal of tobacco-specific nitrosamines, NNK using metal (Ni and Pb)-doped single walled carbon nanotubes as an adsorbent. These investigations have been carried using first-principle calculations, molecular orbital theory, natural bond orbital analysis, DFT framework, etc. Herein, we report an experimental work on removing the particulate matter, heavy metals, nicotine, and tar carcinogens from cigarette smoke using multiwalled carbon nanotube membrane.

Membrane technology has emerged as a dignified separation technology in the last few decades and is presently in the state of rapid growth and innovation.<sup>46–48</sup> At present, many different membrane separation technologies have been developed and are being used in an impressive variety of applications such as wastewater treatment,<sup>49</sup> air cleaning,<sup>22</sup> gas separation, etc.<sup>50</sup> Among these separation processes, the wastewater treatment and air cleaning technology has advanced with remarkable frequency. However, the membrane based gas separation technology is still in its infancy and significant improvements are needed in many aspects such as

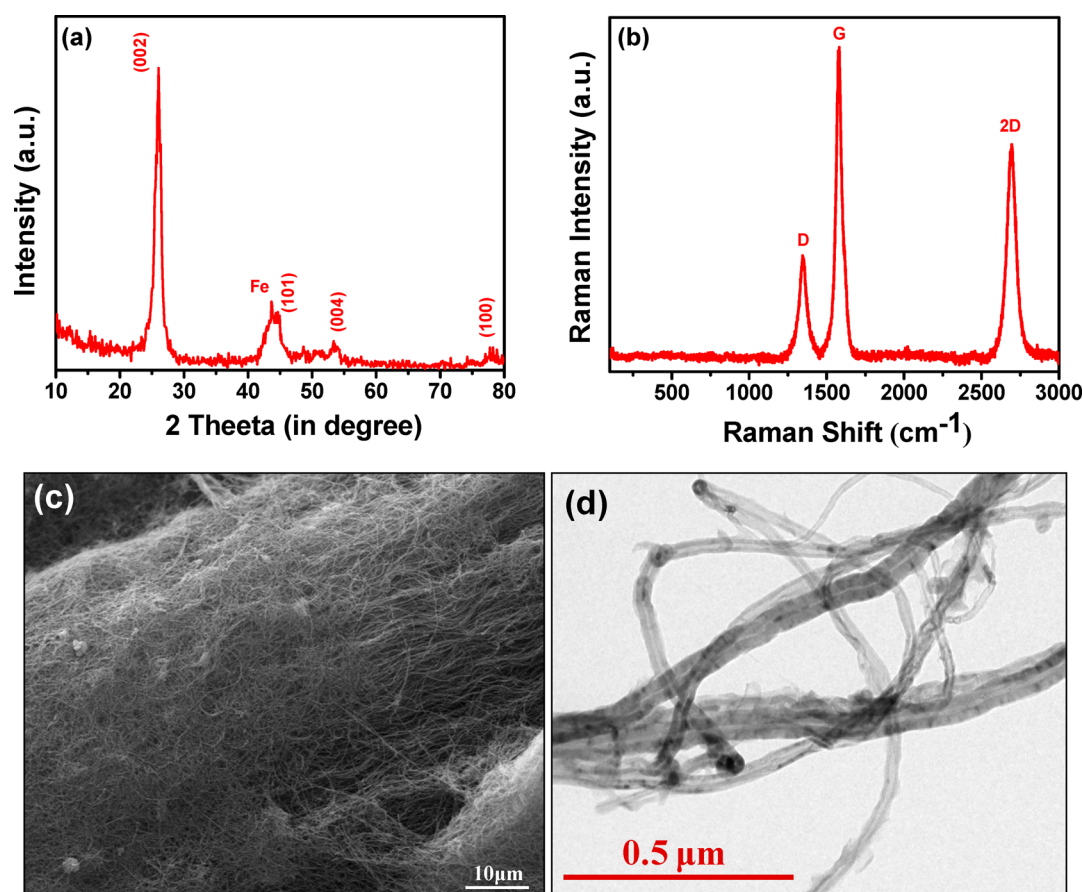


**Figure 2.** (a) Typical XRD patterns of the as-synthesized MWCNTs; (b) Raman spectra of MWCNTs; (c) SEM image showing uniform and dense formation of MWCNTs; (d) TEM image of MWCNTs with average diameter of 50 nm.

the development of new membrane materials with higher selectivity, permeability, and fabrication methods.

Carbon nanotubes (CNTs), which are well-known for their high aspect ratio, large surface area, high thermal stability, and entangled open tubular networks, have been well studied as a pollutant absorber in the past few decades.<sup>29,51,52</sup> In addition to this, the several attempts have also been made to reduce the toxicity of cigarette smoke using the powder form of nanotubes.<sup>29,36</sup> Thus, we believe that a MWCNTs membrane could be the promising candidate for removing toxic compounds from cigarette smoke. Interestingly, to the best of our knowledge, the removal of toxic compounds from the cigarette smoke by such a type of lightweight, flexible, binder-free membrane has not been reported yet. Therefore, keeping the above aspects in mind, we attempted to remove toxic compounds from cigarette smoke using a MWCNTs membrane and found better results than the earlier reported works.<sup>29,32–36</sup>

In this work, we report the fabrication of a novel cigarette filter, developed by the insertion of a monolithic, self-supporting, lightweight ( $\sim 0.0013$  g), binder-free, flexible, and hydrophobic MWCNTs membrane into the conventional cellulose acetate filter. This cigarette filter shows a high filtering efficiency of  $\sim 99\%$  for  $\text{PM}_{2.5}$ . The developed filter is also capable of removing other toxic chemicals/compounds like tar, nicotine, and heavy metals (here Pb has been chosen as model element in view of its acute toxic risk) from mainstream smoke. The approximate cost of materials for the preparation of 1000 filters (diameter  $\sim 0.830$  cm) is INR  $\sim 75$  ( $\sim 1.05$  USD).

## 2. EXPERIMENTAL SECTION

**2.1. Materials.** Moments cigarette (VST Industries Limited, India) has been used as a model cigarette for all investigations. Ferrocene ( $\text{C}_{10}\text{H}_{10}\text{Fe}$ ) has been procured from Alfa Aesar, India. Toluene ( $\text{C}_7\text{H}_8$ ), acetone ( $\text{C}_3\text{H}_6\text{O}$ ), and methanol ( $\text{CH}_3\text{OH}$ ) have been purchased from Molychem, India. All chemicals were of analytical grade and used as received.

**2.2. Synthesis of MWCNTs.** MWCNTs were synthesized inside the quartz tubing furnace maintained at  $850^\circ\text{C}$  by spraying the homogeneous solution of ferrocene and toluene under the constant flow of argon gas as shown in Figure S1.<sup>51,53</sup> After the exposure of spray pyrolysis, quartz tubing was cooled under the flow of argon gas at ambient temperature. Thereafter, a thick black film made of MWCNTs formed inside the quartz tube and was collected.

**2.3. Preparation of MWCNTs Membrane.** 0.4 g of as-synthesized MWCNTs was dispersed in 100 mL of acetone using a high speed homogenizer. Thereafter, the well dispersed suspension of MWCNTs was filtered using a specially designed vacuum-assisted filtration unit. A uniform black film deposited over the Whatman filter paper dried at  $55^\circ\text{C}$  for 30 min. After that the self-supporting flexible film was peeled off and cut into the desired shapes for further testing as a cigarette filter. The schematic of the overall procedure has been shown in Figure 1.

**2.4. Instrumentation and Methods.** The cigarettes were first conditioned for 48 h in air at  $(25 \pm 2)^\circ\text{C}$  before performing the experiment. The experiment was performed by a self-assembled smoking system (as shown in Figure S2), which was set with 40 mL per second of puffing volume.

To quantify the size of particles distributed in the cigarette smoke, we used two particle sizer spectrometers: (i) optical particle sizer (TSI, model-3330, USA) and (ii) Nanoscan SMPS nanoparticle sizer (TSI, model-3910, USA) along with two particle concentration

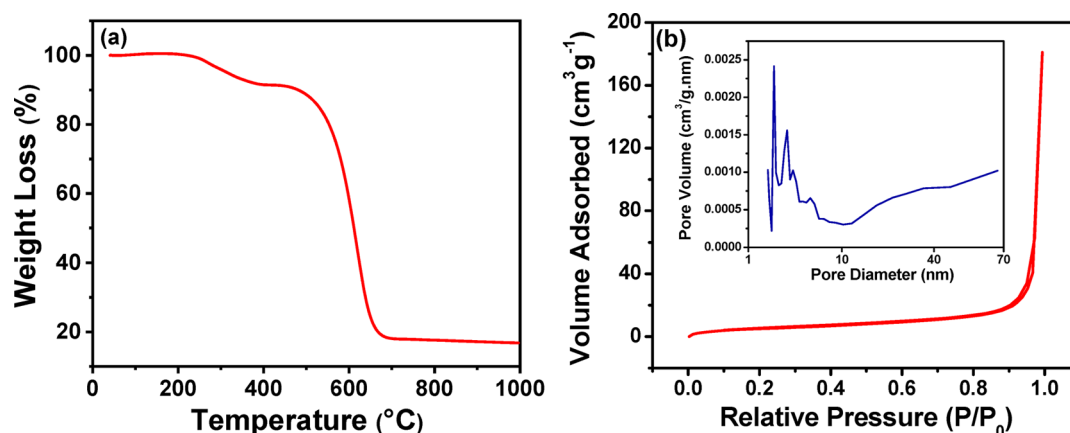


**Figure 3.** (a) Typical TGA curve of the fabricated MWCNTs membrane; (b)  $N_2$  adsorption/desorption isotherms obtained for fabricated MWCNTs membrane (the inset shows the corresponding pore size distribution).

diluters (TSI, model-3332, USA). Thus, the number, surface area, and mass concentration of particles in the cigarette smoke were recorded in all diameters.

Further, to determine the concentration of nicotine and heavy metal species in the cigarette smoke, the mainstream of cigarette smoke was directed to flow into a gas impinger filled with 30 mL of methanol as shown in Figure S2. Thereafter, dissolved nicotine and heavy metal species were collected and analyzed using a UV-vis absorption spectrometer (PerkinElmer, USA) and Optima 7000 DV inductively coupled plasma optical emission spectrometer (ICP-OES) system (PerkinElmer, USA) respectively.

**2.5. Determination of Removal Efficiency.** The removal efficiency of PM, nicotine and heavy metals has been calculated by following expression:

$$\eta(\%) = \left( \frac{\sum n - n}{\sum n} \right) \times 100$$

where  $\eta$  is the removal efficiency. The term  $\sum n$  represents the total concentration of PM, nicotine, and heavy metal species present in smoke before filtration, i.e., with conventional cellulose acetate filter, and the term  $n$  represents the concentration of PM, nicotine, and heavy metals species present in smoke after filtration, i.e., with the filter developed in this work.

### 3. RESULTS AND DISCUSSION

The structural and morphological characterizations were carried out using an X-ray diffractometer (PANalytical, UK), scanning electron microscope (SEM) (ZEISS, Germany), transmission electron microscope (TEM) (TECNAI 20 G<sup>2</sup>) operated at accelerating voltage of 200 kV, and an atomic force microscope (AFM) Park XE7 (Park, South Korea). The spectroscopic characterizations were carried out using a Raman microscope (Renishaw inVia, Germany), Fourier transform infrared (FTIR) spectrometer (Frontier, PerkinElmer, USA), and UV-vis absorption spectrometer (PerkinElmer, USA). The thermogravimetric analysis (TGA) and specific surface area measurements were carried out using an 851e thermal analysis instrument (Mettler Toledo) and Gemini VII 2390 surface area analyzer (Micromeritics, US), respectively.

**3.1. Characterization of as-Synthesized MWCNTs.** To confirm the structure of as synthesized sample, X-ray powder diffraction was carried out using an X-ray diffractometer with Cu-K $\alpha$  radiation. Figure 2a shows the typical XRD pattern of as synthesized sample. The pattern displayed an intense diffraction peak around  $2\theta = 26^\circ$  and low intense diffraction peaks around  $44^\circ$ ,  $53^\circ$ , and  $78^\circ$ , which correspond to the planes (002), (101), (004), and (100), respectively, have been

successfully indexed with JCPDS Card No. 751621. Also, the low intense diffraction peak around  $2\theta = 43^\circ$  corresponds to the Fe (JCPDS Card No. 654150) present within the MWCNTs used as the catalyst during synthesis. This result indicates that the as synthesized samples are pure and well graphitized hexagonal structures.

It is well-known that Raman spectra provide the information about the purity, defects, and tube alignment and help in the distinction of the presence of MWCNTs relative to other carbon allotropes. Therefore, for further structural conformation, Raman spectra of a synthesized sample have been recorded using 532 nm laser excitation (Figure 2b). The Raman spectra consist of a peak around  $1343\text{ cm}^{-1}$  called the “D” band, which is due to the scattering from local defects or the disorders present in the synthesized MWCNTs. Another two peaks around  $1582\text{ cm}^{-1}$ , called “G” band, and around  $2695\text{ cm}^{-1}$  called the overtone or the second order harmonic of the D band are mainly due to the tangential vibration of C-atoms and two-phonon second-order scattering process, respectively. The intensity ratio of G band to D band ( $I_G/I_D$ ) is found to be about 3.09, which confirms the high quality of the sample, i.e., no amorphous carbon present in the sample.

Figure 2c shows the SEM image of the synthesized MWCNTs, which clearly show the bulk formation of good quality, entangled tube-like structure with a high aspect ratio. The TEM image (Figure 2d) reveals that the synthesized tubes are multiwalled in nature having an average diameter of 50 nm. The TEM image also shows the presence of the Fe catalyst at the tip, used during the synthesis of MWCNTs. This shows good agreement with previous results.

**3.2. Characterization of MWCNTs Membrane.** To understand the thermal behavior of the fabricated MWCNTs membrane, TGA studies were carried out. Figure 3a shows the typical TGA curve of the fabricated MWCNTs membrane, which clearly indicates that the initiation of weight loss takes place around  $230\text{ }^\circ\text{C}$  followed by a sharp weight loss around  $500\text{ }^\circ\text{C}$ . The weight loss around  $230\text{ }^\circ\text{C}$  takes place due to the moisture present in the sample.<sup>54–57</sup> However, the sharp weight loss starting around  $500\text{ }^\circ\text{C}$  is possibly due to the decomposition of nanotubes and little amorphous carbon.<sup>58–60</sup> Thus, the fabricated MWCNTs membrane maintains favorable thermal stability which is necessary for use in cigarettes.

Earlier reports show that the surface area, pore size, and pore volume are the important parameters that influence the removal efficiency of such nanostructured materials.<sup>61</sup> Because

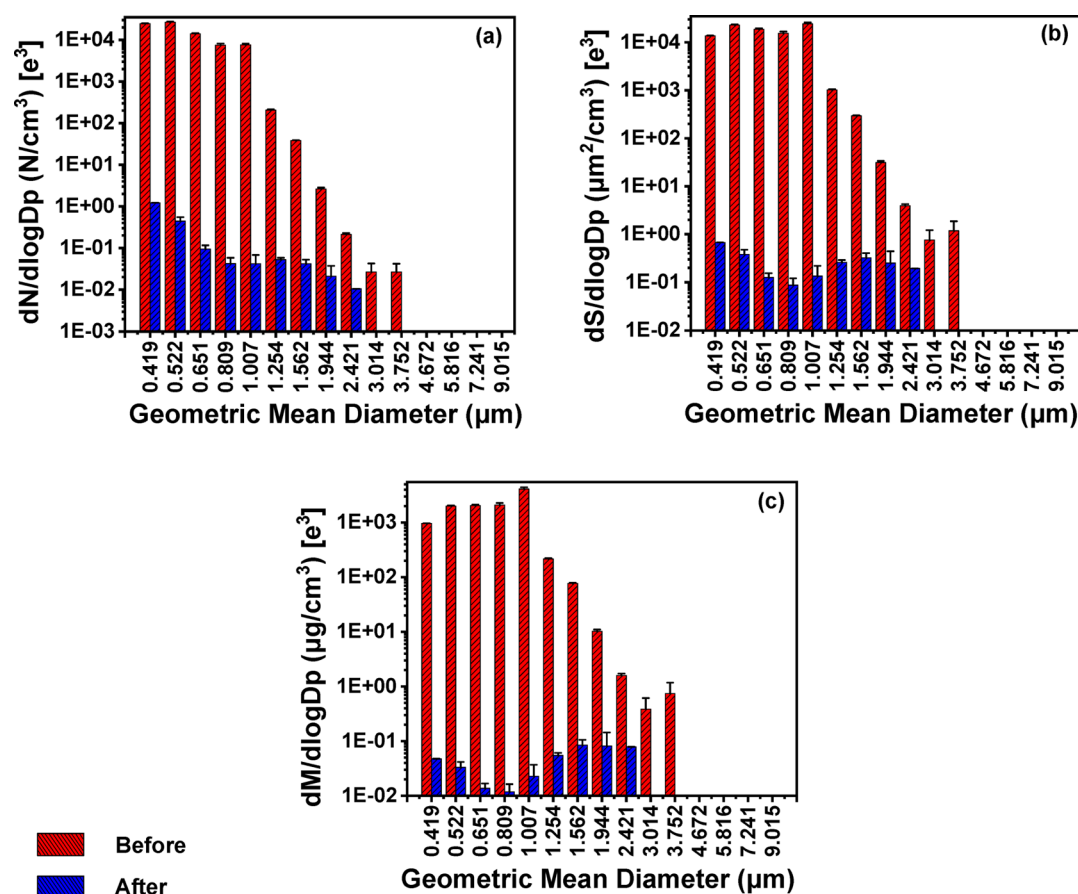


**Figure 4.** Characterizations of number, surface area, and mass concentration of cigarette smoke particles by TSI-3330 optical particle sizer spectrometer. The *x*-axis is the geometric mean diameter of PM in micrometer. The *y*-axis represents the number/surface area/mass concentration of PM in cigarette smoke: (a) number concentration; (b) surface area concentration; (c) mass concentration, of PM in cigarette smoke, before and after employing the fabricated filter, respectively.

the toxic compounds present in cigarette smoke are mainly adsorbed or condensed on the surface or in the hollow cores of such nanostructured materials.<sup>34,36</sup> Hence, to analyze the surface area and porous texture of the fabricated MWCNTs membrane, N<sub>2</sub> adsorption/desorption isotherms were carried out at 77 K as shown in Figure 3b. The figure clearly reveals that the specific surface area of the fabricated MWCNTs membrane is about  $\sim 19.26 \text{ m}^2 \text{ g}^{-1}$ . The inset of Figure 3b shows Barrett–Joyner–Halenda (BJH) pore size distribution curve of the MWCNTs membrane, which clearly shows that the average pore diameter of the MWCNTs membrane is about  $\sim 16.37 \text{ nm}$ .

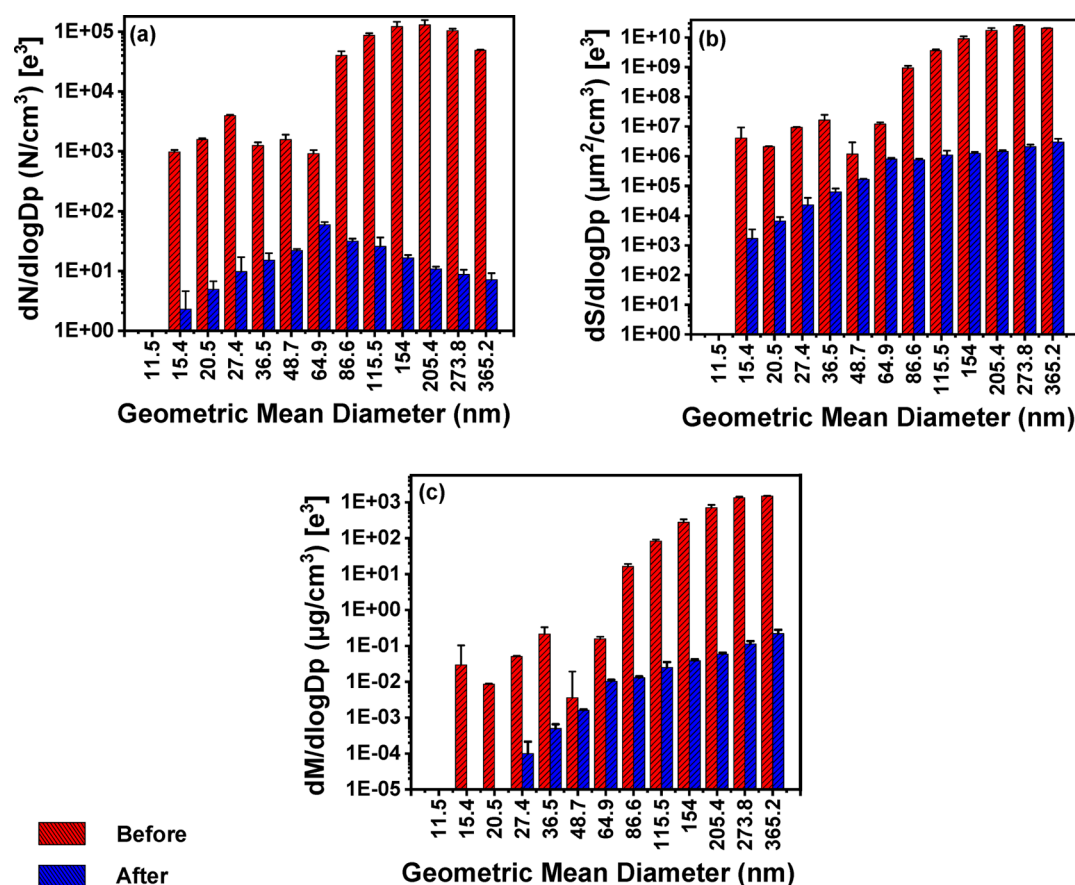
**3.3. Analysis of Total Particulate Matter in the Cigarette Smoke, before and after Filtration by the Fabricated Filter.** In recent years the optical particle sizer spectrometer and nanoscan SMPS nanoparticle sizer spectrometer are well established and accepted characterization techniques for the determination of particulate matter concentration in air and smoke.<sup>62–64</sup> Thus, to investigate the concentration of total particulate matter (TPM) in the cigarette smoke before and after employing the fabricated filter, a series of experiments were carried using an optical particle sizer spectrometer and nanoscan SMPS nanoparticle sizer spectrometer simultaneously, and the results were found to be similar.

Figure 4 panels a, b, and c represents the number, surface area, and mass concentration of PM having geometric mean

diameter (GMD) in micrometer ( $\mu\text{m}$ ), before and after employing the fabricated filter, respectively. As shown in Figure 4a, the smoke from a cigarette with conventional cellulose acetate filter comprises a high average of number concentration,  $\sim 8.945 \times 10^6 \text{ N/cm}^3$  of the PM, the GMD of which is in the range 0.419 to 2.421  $\mu\text{m}$ , also PM having a GMD greater than 2.421  $\mu\text{m}$  has also been detected significantly  $\sim 0.008 \times 10^3 \text{ N/cm}^3$  in the smoke of cigarettes with the conventional cellulose acetate filter. However, after employing the fabricated filter, it has been found that the average number concentration of PM having GMD in between 0.419 to 2.421  $\mu\text{m}$  reduces drastically to  $\sim 0.217 \times 10^3 \text{ N/cm}^3$ , whereas the PM having GMD greater than 2.421  $\mu\text{m}$  could not be detected in the cigarette smoke due to the addition of the particle concentration diluter and low concentration itself.

Similarly, Figure 4 panels b and c shows the surface area and mass concentration of PM having a GMD value in micrometer, before and after employing the fabricated filter. This clearly reveals that the PM with GMD in between 0.419 to 2.421  $\mu\text{m}$  also possesses an extremely high average surface area and mass concentration of about  $\sim 1.069 \times 10^7 \mu\text{m}^2/\text{cm}^3$  and  $\sim 1.280 \times 10^6 \mu\text{g}/\text{cm}^3$ , respectively. After employing the fabricated filter the average concentration of the PMs reduces drastically to the value  $\sim 0.269 \times 10^3 \mu\text{m}^2/\text{cm}^3$  and  $\sim 0.047 \times 10^3 \mu\text{g}/\text{cm}^3$ , respectively.

Similarly, Figure 5 panels a–c represent the number, surface area, and mass concentration of PM having GMD in



**Figure 5.** Characterizations of number, surface area, and mass concentration of cigarette smoke particles by TSI-3910 nanoscan SMPS nanoparticle sizer. The *x*-axis is the geometric mean diameter of PM in nanometers. The *y*-axis represents the number/surface area/mass concentration of PM in cigarette smoke: (a) number concentration; (b) surface area concentration; (c) mass concentration, of PM in cigarette smoke, before and after employing the fabricated filter, respectively.

**Table 1.** Characterizations of Number, Surface Area, and Mass Concentration of Cigarette Smoke Particles with the Diameter  $< 10 \mu\text{m}$ , before (i.e. with Conventional Cellulose Acetate Filter) and after (i.e. with Fabricated Filter in This Work) Employing the Fabricated Filter<sup>a</sup>

cigarette smoke	PM	mean $\pm$ SD		
		no. concn ( $\times 10^3 \text{ N/cm}^3$ )	surface concn ( $\times 10^9 \mu\text{m}^2/\text{cm}^3$ )	mass concn ( $\times 10^3 \mu\text{g}/\text{cm}^3$ )
before	PM <sub>10</sub>	0.007 $\pm$ 0.005	0.239 $\pm$ 0.188	0.129 $\pm$ 0.109
	PM <sub>2.5</sub>	4.22 $\times 10^4 \pm$ 5081.28	5550 $\pm$ 585	1165.315 $\pm$ 72.252
	PM <sub>0.1</sub>	6981.09 $\pm$ 1002.33	140.8 $\pm$ 23.0	2.402 $\pm$ 0.390
after	PM <sub>10</sub>	ND	ND	ND
	PM <sub>2.5</sub>	6.23 $\pm$ 1.24	0.751 $\pm$ 0.141	0.075 $\pm$ 0.016
	PM <sub>0.1</sub>	18.56 $\pm$ 3.37	0.219 $\pm$ 0.026	0.0030 $\pm$ 0.0003

<sup>a</sup>Note: values are given as mean  $\pm$  standard deviation ( $n = 3$ ) and ND represents not detectable due to the extremely low concentration.

nanometer (nm), before and after employing the fabricated filter, respectively. As shown in Figure 5a, the smoke from a cigarette with the conventional cellulose acetate filter, possesses a high average number concentration of  $\sim 4.163 \times 10^7 \text{ N/cm}^3$  of PM with all possible GMD ranges from 11.5 to 365 nm. However, after the fabricated filter was employed, the concentration of these particles were found to be very low at  $\sim 1.655 \times 10^4 \text{ N/cm}^3$ . Similarly, Figure 5 panels b and c show the surface area and mass concentration of PM having a GMD in nanometers, before and after employing the fabricated filter, respectively, which shows similar results as obtained for the number concentration.

The results obtained from optical particle sizer spectrometer and nanoscan SMPS nanoparticle sizer spectrometer in different concentrations have been summarized in tabular form as shown in Table 1.

As shown in above in Table 1, it has been clearly seen that the cigarette smoke is mainly composed of PM<sub>2.5</sub>, which is the main cause of smoke related carcinogenic and deadly diseases. The effect of using a fabricated filter is an enormous reduction in the concentration of this PM<sub>2.5</sub> by  $\sim 99\%$ . Also, the mainstream of smoke contains a significant amount of PM<sub>0.1</sub> and PM<sub>10</sub>, but after using the fabricated filter the concentration of PM<sub>0.1</sub> is hardly detected, while PM<sub>10</sub> is not detected due

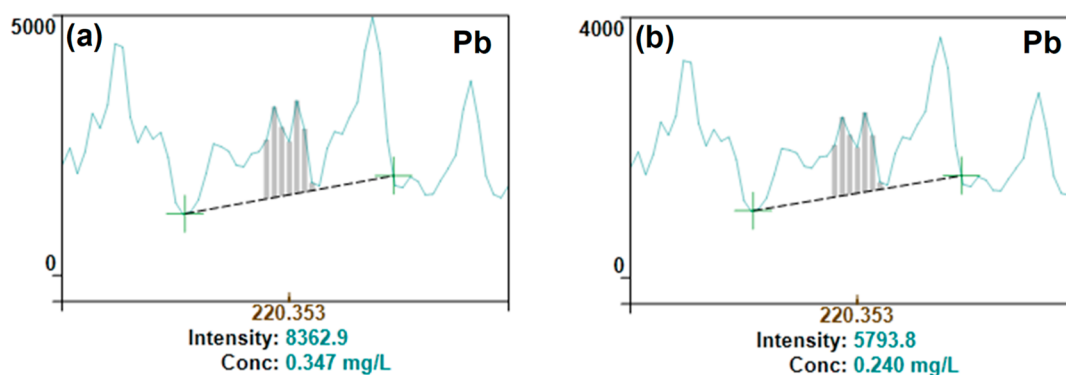


**Figure 6.** ICP-OES spectra of the heavy metal lead presented in the cigarette smoke (a) before (b) after employing the fabricated filter.

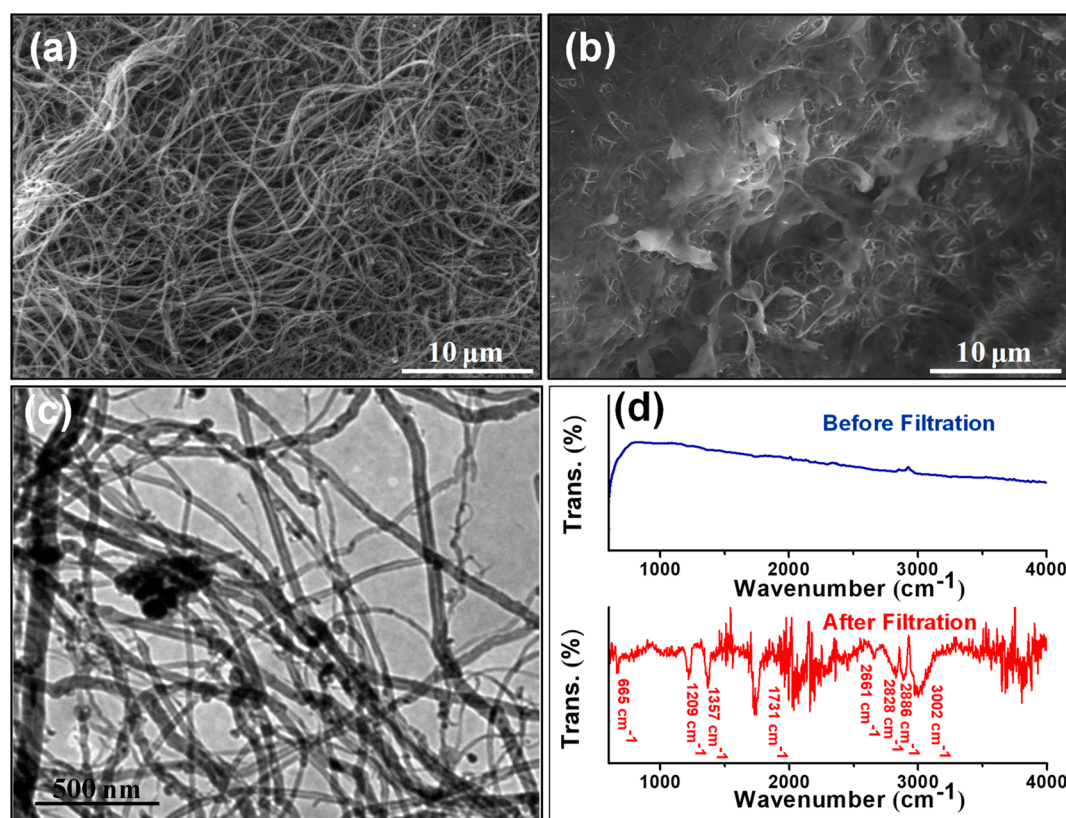


**Figure 7.** (a) SEM image of fabricated MWCNTs membrane before smoking; (b) SEM image of MWCNTs membrane after smoking; (c) TEM image of MWCNTs membrane after smoking; (d) FTIR spectra of MWCNTs membrane before and after the filtration of cigarette smoke.

the use of a particle concentration diluter as well as itself having a very low concentration in smoke.

**3.4. Detection of Heavy Metal Concentration in Cigarette Smoke.** When a smoker smokes, the heavy metals present in the cigarette's tobacco are either left in the cigarette filter or enter into the smoker's body or spread into the air through smoke. Since the heavy metals which remain in the cigarette filter or entered into the smoker's body are directly related to the health of the smoker, it becomes very necessary to study also these metals. Therefore, to investigate the heavy metals concentration in the cigarette smoke, ICP-OES measurement has been carried out. In this measurement Pb has been chosen as the model element in view of its acute toxic risk.

Figure 6 shows the result obtained from the ICP-OES measurement. From Figure 6a, the intensity of the ICP curve

at 220.353 nm has been found around 8362.9, which corresponds to the 0.347 mg/L of Pb heavy metal in cigarette smoke when the conventional cellulose acetate filter is used. Whereas, after using the fabricated filter, the concentration of Pb heavy metal decreases significantly to 0.240 mg/L (as shown in Figure 6b), which is around 30% less than its initial concentration. This clearly indicates that the fabricated cigarette filter possesses significantly enhanced capability to remove the heavy metals from cigarette smoke as compared to the conventional cellulose acetate filter.

**3.5. Analysis of Nicotine Concentration in Cigarette Smoke.** Further, to investigate the removal efficiency of the fabricated filter for nicotine, UV-vis absorption spectra of cigarette smoke has been recorded before and after employing the fabricated filter as shown in Figure S3. The absorption spectra of cigarette smoke with conventional cellulose acetate

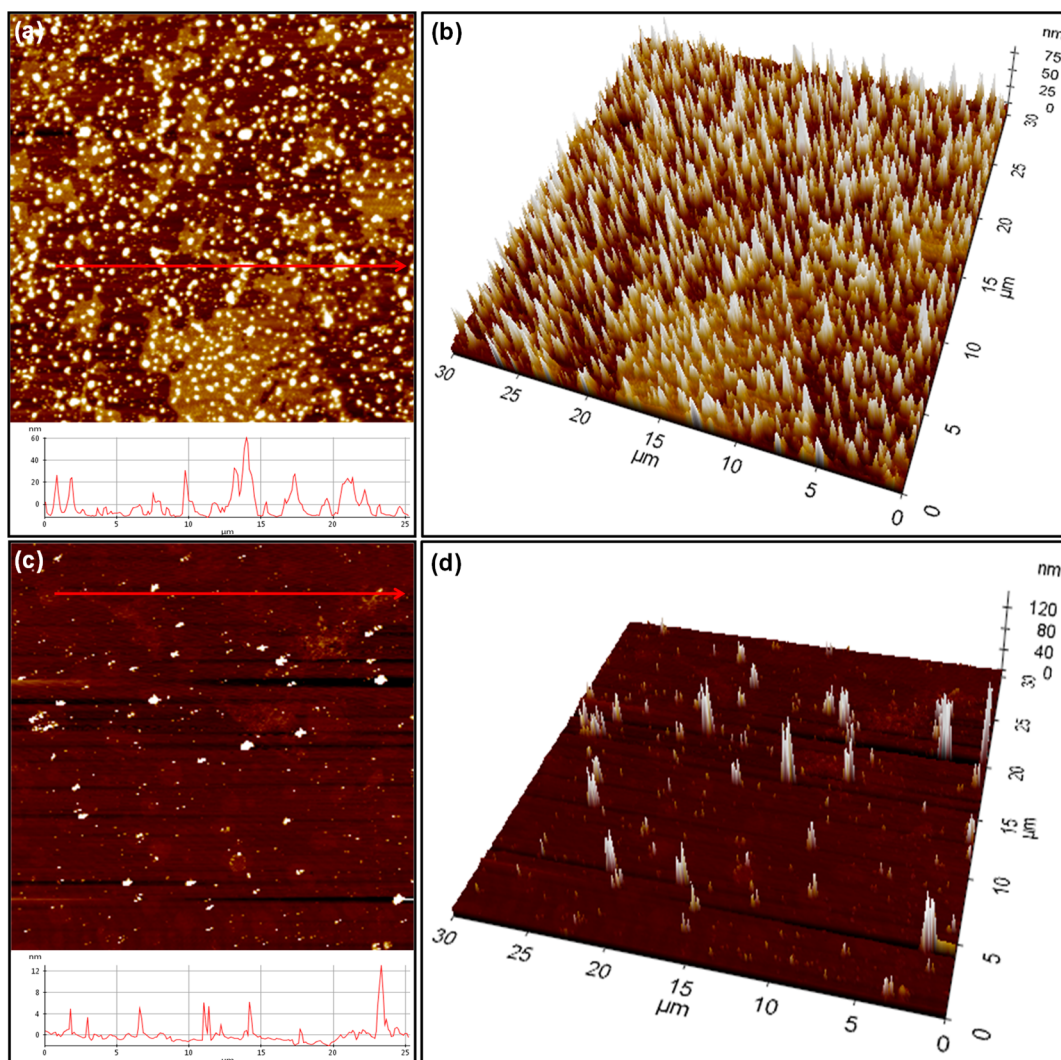


**Figure 8.** (a) 2D and (b) 3D topography of smoke particles with conventional cellulose acetate filter; (c) 2D and (d) 3D topography of smoke particle with fabricated filter. The height profiles recorded along the red arrow are shown in the insets of panels a and c.

filter possess a broad absorption band around  $\sim 263$  nm, which corresponds to the absorption peak of nicotine present in smoke.<sup>65</sup> However, in the absorption spectra of smoke filtered with the fabricated filter, this absorption band has nearly disappeared, which indicates that nicotine present in cigarette smoke has been significantly adsorbed by the MWCNTs membrane inserted in the conventional cellulose acetate filter. This adsorption phenomenon was strongly favored via the molecule–nanotube interaction, which has been carried by the tri-coordinated nitrogen atom from the nicotine.<sup>66</sup>

This excellent removal efficiency of the fabricated filter is presumably related to its intrinsic physical and chemical adsorption properties. Earlier, Branton et al.<sup>61</sup> and Yu et al.<sup>29</sup> have reported that the adsorption efficiency of additive filter materials increases almost linearly with the specific surface area and its geometrical length. Herein, the specific surface area of the MWCNTs membrane is comparable to or higher than the other additive materials used to develop the filter. In addition, this MWCNTs membrane also possesses a randomly oriented concentric open tubular network with high aspect ratio nanotubes entangled to each other. This provides geometrical confinement for toxic chemicals/compounds present in the mainstream of cigarette smoke. Along with these, one of the

most important property of the nanotubes is its internal diameters, which are comparable in size to that of many small toxic molecules, which raises the prospects of size-based exclusion and separation of these toxic molecules. Furthermore, the inserted flexible membrane is also very thin ( $\sim 0.16$  mm) and porous, which allows the cigarette smoke to pass easily through it. Also, the smoking regimes used during the measurements and the typical measured pressure drop ( $\sim 143.5$  Pa) across the filter suggest that the draw filter resistance is quite fine and favorable for smoking. Thus, we believe that it may also be practically acceptable.

Therefore, for further confirmation, the microstructural characterizations of the inserted MWCNTs membrane, before and after the passage of smoke, have been carried out. Figure 7 panels a and b show the SEM image of the inserted MWCNTs membrane before and after smoking, respectively. As shown in Figure 7a, before smoking, the surface of the inserted MWCNTs membrane is apparently clear and has randomly oriented tubular nanostructures which are entangled to each other. However, after smoking, the surface of the inserted membrane is fully covered with PM and tar forming jelly-like structures as shown in Figure 7b, which indicates that its use in traditional filters is promising. Figure 7c shows the TEM image

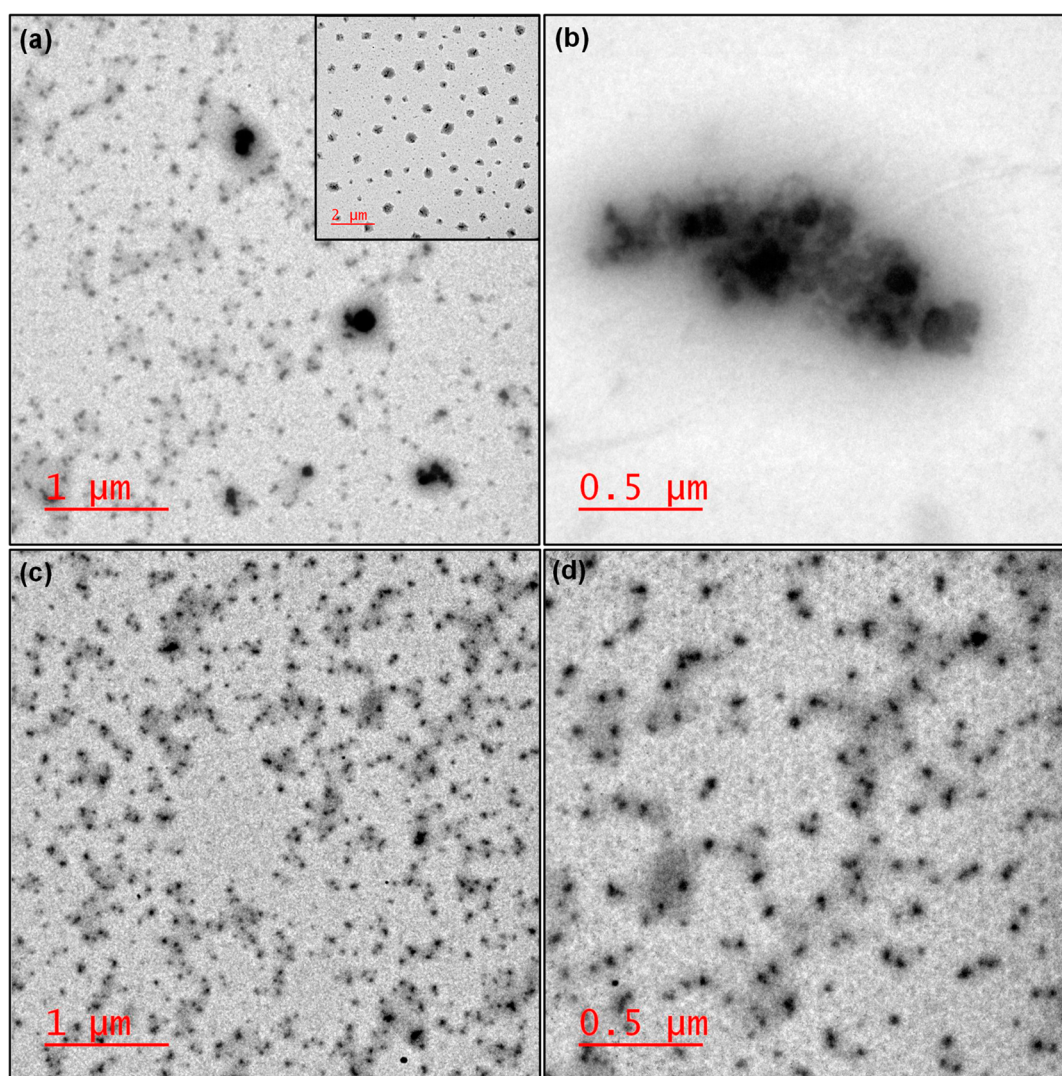


**Figure 9.** (a,b) TEM images of PM filtered with conventional cellulose acetate filter; (c,d) TEM images of PM filtered with fabricated filter.

of MWCNTs membrane after smoking. From this, it has been clearly observed that the few particles are adsorbed or condensed on it after smoking. Thus, we believe that the geometrical structure of nanotubes and the adsorption behavior of the membrane surface both are useful in the filtration process. However, the voids between the nanotubes dominate the hollow cores. Nevertheless, we cannot completely disregard the fact that there might be some toxins adsorbed or condensed in the hollow cores of the nanotubes, but the exact distribution is very difficult to depict. Thus, most of the filtration occurs from voids between the nanotubes. These conclusions are well supported by the earlier reported works.<sup>36,51</sup>

Figure 7d shows the FTIR spectra of the inserted membrane before and after smoking. By comparing these two FTIR spectra, it can be clearly seen that the inserted MWCNTs membrane has no absorption peak before smoking, whereas after smoking, some absorption peaks have been introduced in the spectra of the inserted membrane. The absorption peaks appear approximately at  $3002\text{ cm}^{-1}$ ,  $2886\text{ cm}^{-1}$ ,  $2828\text{ cm}^{-1}$ , and  $1731\text{ cm}^{-1}$  and correspond to the Ar–H stretch, –OH dimer, C–H stretch, and C=O stretching vibrations, respectively. This indicates the presence of many new groups such as methylene, methine, aldehyde, etc. introduced over the

surface of the membrane, that came from nicotine, benzaldehyde, and other hydrocarbons present in the cigarette smoke. Also, the absorption peaks appearing approximately at  $1209\text{ cm}^{-1}$  and  $1357\text{ cm}^{-1}$  correspond to the C–O stretch and N–O symmetric stretch, respectively, which may come from carboxyl groups and nitro compounds. The other absorption peaks appear with significant absorption intensity approximately at  $2661\text{ cm}^{-1}$  and  $665\text{ cm}^{-1}$  indicating that a large number of toxic compounds have been adsorbed by the inserted MWCNTs membrane.

In recent years, AFM has become a very powerful tool because of its potential applications in imaging and measuring matter at the nanoscale level with high resolution. Therefore, to endorse the removal of PM by other methods, AFM measurement was carried out in noncontact mode to visualize the surface topography of PM before and after employing the fabricated filter, as shown in Figure 8. Figure 8 panels a and b represent the 2D and 3D topography of PM before employing the fabricated filter, i.e., with the conventional cellulose acetate filter, which shows the existence of an extremely high concentration of PM with variable shapes and sizes. The height profile (shown in the inset of Figure 8a) recorded along the red arrow shows the major changes in the height of PM, which suggest that the smoke from a cigarette with a

conventional filter possesses an enormously high concentration of PM in variable shapes, sizes, and heights. Figure 8 panels c and d represent the 2D and 3D topography of cigarette smoke particle filtered with the fabricated filter, respectively. From here, we can clearly observe that after using the fabricated filter the concentration of PM is reduced drastically and the height profile (as shown in the inset of Figure 8c) recorded along the red arrow shows nearly uniform distribution in the heights of PM.

Further, the microstructures of the PM in the cigarette smoke before and after employing the fabricated filter has also been investigated using TEM as shown in Figure 9. Figure 9 panels a and b show the TEM images of cigarette smoke particles filtered with the conventional cellulose acetate filter at different magnifications. This clearly reveals that the smoke from cigarettes with a conventional cellulose acetate filter possesses variable sizes of PM, the lateral dimensions of which vary from  $\sim 15$  nm to  $\sim 2$   $\mu$ m and more. Whereas, after employing the fabricated filter, PM with smaller lateral dimensions ranging from  $\sim 15$  nm to  $\sim 80$  nm have mostly been observed as shown in Figure 9 panels c and d. This result has also been well supported by the other reported works.<sup>67,68</sup>

The results obtained from AFM and TEM measurements also reveal that the cigarette smoke does not contain nanotubes in its mainstream after the incorporation of fabricated filter. Thus, we believe that the use of a carbon nanotube membrane in a conventional cellulose acetate filter has not put any adverse effect on human health.

The comparison of the present work with other reported works (shown in Table 2) suggests that the fabricated filter is

**Table 2. A Comparison of the Proposed Work with Other Reported Works for the Removal of Various Hazards Compounds from the Cigarette Smoke**

serial no.	adsorbent materials	target	removal efficiency (%)	ref
1	lyophilized carbon nanotubes/graphene oxide	heavy metals	63–79	29
2	zeolite-like calcosilicate	nitrosamines	30–60	32
3	chitosan	heavy metals	16–55	33
4	carbon nanocages	phenolic compounds and PM	55–75	34
5	carbon nanotubes mixture	tar, nicotine, benzo[a]pyrene, phenolic compounds	20–35	35
6	oxidized carbon nanotubes	tar	38–72	36
7	titanate nanosheets and nanotubes	nicotine, tar and volatile organic compounds	1.1–97.3	37
8	electrospun nanofibers	tar	47.7–71.6	69
9	MWCNTs membrane	heavy metals, tar and nicotine PM <sub>2.5</sub>	$\sim 30$ $\sim 99$	present work

highly efficient for the purpose of filtering more toxic chemicals/compounds such as PM, nicotine, tar, and heavy metals from cigarette smoke.

#### 4. CONCLUSION

In summary, a novel cigarette filter has been developed by the insertion of a monolithic, self-supporting, lightweight ( $\sim 0.0013$

g), binder-free, flexible, and hydrophobic MWCNTs membrane into the conventional cellulose acetate filter. This flexible MWCNTs membrane has been fabricated using a simple vacuum-assisted filtration technique followed by the synthesis of MWCNTs using a cost-effective spray pyrolysis technique. The various characterization techniques such as XRD, Raman, SEM, TEM, TGA, and BET demonstrated that the fabricated membrane possesses randomly oriented tube-like structures entangled to each other with a high specific surface area and thermal stability. These unique properties of the fabricated membrane have been successfully applied for the development of a cigarette filter. The developed filter offers excellent performance for the elimination of PM<sub>2.5</sub> with a removal efficiency of  $\sim 99\%$ . It also shows significant ability for the removal of nicotine, tar, and toxic heavy metals such as lead present in cigarette smoke, which is comparable to or better than the earlier reported works for smoke filtration. Thus, we believe that the present study will provide a new avenue for the development of an efficient and economical filter for the cigarette.

#### ■ ASSOCIATED CONTENT

##### Supporting Information

The Supporting Information is available free of charge at <https://pubs.acs.org/doi/10.1021/acsanm.9b02277>.

Schematic diagram for MWCNTs synthesis, schematic diagram for smoking system, UV–vis absorption spectra of cigarette smoke (PDF)

#### ■ AUTHOR INFORMATION

##### Corresponding Author

Anchal Srivastava – Banaras Hindu University, Varanasi, India; [orcid.org/0000-0002-6573-5345](https://orcid.org/0000-0002-6573-5345); Phone: +91- 9453203122; Email: [anchalbhu@gmail.com](mailto:anchalbhu@gmail.com)

##### Other Authors

Sumit Kumar Pandey – Banaras Hindu University, Varanasi, India; [orcid.org/0000-0001-7999-3073](https://orcid.org/0000-0001-7999-3073)

Pramod Kumar Vishwakarma – Banaras Hindu University, Varanasi, India; [orcid.org/0000-0001-5330-2959](https://orcid.org/0000-0001-5330-2959)

Sunil Kumar Yadav – Indian Institute of Technology, Banaras Hindu University, Varanasi, India

Prashant Shukla – Indian Institute of Technology, Banaras Hindu University, Varanasi, India

Complete contact information is available at: <https://pubs.acs.org/doi/10.1021/acsanm.9b02277>

##### Notes

The authors declare no competing financial interest.

#### ■ ACKNOWLEDGMENTS

S.K.P. acknowledges UGC, New Delhi, India, for providing a Fellowship. A.S. acknowledges DST, India (DST-Purse Scheme 5050), and DST-SERB India (Project Code: EMR/2016/007720) for providing financial assistance. The authors are also thankful to Interdisciplinary School of Life Sciences, Institute of Science, Banaras Hindu University, Varanasi, India, for ICP-OES measurement.

## REFERENCES

- (1) Bruce, N.; Perez-Padilla, R.; Albalak, R. Indoor air pollution in developing countries: a major environmental and public health challenge. *Bull. World Health Organization* **2000**, *78*, 1078–1092.
- (2) WHO report on the global tobacco epidemic, 2017: monitoring tobacco use and prevention policies; World Health Organization, 2017.
- (3) WHO report on the global tobacco epidemic, 2008: The MPOWER package; World Health Organization, 2008.
- (4) Stedman, R. L. Chemical composition of tobacco and tobacco smoke. *Chem. Rev.* **1968**, *68* (2), 153–207.
- (5) Zevin, S.; Saunders, S.; Gourlay, S. G.; Jacob, P.; Benowitz, N. L. Cardiovascular effects of carbon monoxide and cigarette smoking. *J. Am. Coll. Cardiol.* **2001**, *38* (6), 1633–1638.
- (6) Richter, P.; Pechacek, T.; Swahn, M.; Wagman, V. Reducing levels of toxic chemicals in cigarette smoke: a new Healthy People 2010 objective. *Public Health Rep.* **2008**, *123* (1), 30–38.
- (7) Kim, S. Y.; Sim, S.; Choi, H. G. Active, passive, and electronic cigarette smoking is associated with asthma in adolescents. *Sci. Rep.* **2017**, *7* (1), 17789.
- (8) Stämpfli, M. R.; Anderson, G. P. How cigarette smoke skews immune responses to promote infection, lung disease and cancer. *Nat. Rev. Immunol.* **2009**, *9* (5), 377.
- (9) Jha, P. Avoidable global cancer deaths and total deaths from smoking. *Nat. Rev. Cancer* **2009**, *9* (9), 655.
- (10) Hopkin, J.; Evans, H. Cigarette smoke-induced DNA damage and lung cancer risks. *Nature* **1980**, *283* (5745), 388.
- (11) Marugame, T.; Sobue, T.; Nakayama, T.; Suzuki, T.; Kuniyoshi, H.; Sunagawa, K.; Genka, K.; Nishizawa, N.; Natsukawa, S.; Kuwahara, O.; Tsubura, E. Filter cigarette smoking and lung cancer risk; a hospital-based case–control study in Japan. *Br. J. Cancer* **2004**, *90* (3), 646.
- (12) Moreno-Gonzalez, I.; Estrada, L. D.; Sanchez-Mejias, E.; Soto, C. Smoking exacerbates amyloid pathology in a mouse model of Alzheimer's disease. *Nat. Commun.* **2013**, *4*, 1495.
- (13) Thun, M. J.; Henley, S. J.; Calle, E. E. Tobacco use and cancer: an epidemiologic perspective for geneticists. *Oncogene* **2002**, *21* (48), 7307.
- (14) Pleasance, E. D.; Stephens, P. J.; O'Meara, S.; McBride, D. J.; Meynert, A.; Jones, D.; Lin, M.-L.; Beare, D.; Lau, K. W.; Greenman, C.; et al. A small-cell lung cancer genome with complex signatures of tobacco exposure. *Nature* **2010**, *463* (7278), 184.
- (15) Seinfeld, J. H. Urban air pollution: state of the science. *Science* **1989**, *243* (4892), 745–752.
- (16) Zhang, R.; Jing, J.; Tao, J.; Hsu, S.-C.; Wang, G.; Cao, J.; Lee, C. S. L.; Zhu, L.; Chen, Z.; Zhao, Y.; Shen, Z. Chemical characterization and source apportionment of PM 2.5 in Beijing: seasonal perspective. *Atmos. Chem. Phys.* **2013**, *13* (14), 7053–7074.
- (17) Maricq, M. M. Chemical characterization of particulate emissions from diesel engines: A review. *J. Aerosol Sci.* **2007**, *38* (11), 1079–1118.
- (18) Kim, K.-H.; Kabir, E.; Kabir, S. A review on the human health impact of airborne particulate matter. *Environ. Int.* **2015**, *74*, 136–143.
- (19) Pope III, C. A.; Dockery, D. W. Health effects of fine particulate air pollution: lines that connect. *J. Air Waste Manage. Assoc.* **2006**, *56* (6), 709–742.
- (20) Brook, R. D.; Rajagopalan, S.; Pope III, C. A.; Brook, J. R.; Bhatnagar, A.; Diez-Roux, A. V.; Holguin, F.; Hong, Y.; Luepker, R. V.; Mittleman, M. A.; et al. Particulate matter air pollution and cardiovascular disease: an update to the scientific statement from the American Heart Association. *Circulation* **2010**, *121* (21), 2331–2378.
- (21) Anenberg, S. C.; Horowitz, L. W.; Tong, D. Q.; West, J. J. An estimate of the global burden of anthropogenic ozone and fine particulate matter on premature human mortality using atmospheric modeling. *Environ. Health Perspect.* **2010**, *118* (9), 1189–1195.
- (22) Liu, C.; Hsu, P.-C.; Lee, H.-W.; Ye, M.; Zheng, G.; Liu, N.; Li, W.; Cui, Y. Transparent air filter for high-efficiency PM 2.5 capture. *Nat. Commun.* **2015**, *6*, 6205.
- (23) Pappas, R.; Polzin, G.; Zhang, L.; Watson, C.; Paschal, D.; Ashley, D. Cadmium, lead, and thallium in mainstream tobacco smoke particulate. *Food Chem. Toxicol.* **2006**, *44* (5), 714–723.
- (24) Bernhard, D.; Rossmann, A.; Wick, G. Metals in cigarette smoke. *IUBMB Life* **2005**, *57* (12), 805–809.
- (25) Kalcher, K.; Kern, W.; Pietsch, R. Cadmium and lead in the smoke of a filter cigarette. *Sci. Total Environ.* **1993**, *128* (1), 21–35.
- (26) Daff, M.; Kennaway, E.-L. The arsenic content of tobacco and of tobacco smoke. *Br. J. Cancer* **1950**, *4* (2), 173.
- (27) Viroonudomphol, D.; Suwanton, L.; Pinyosirikul, U.; Satsue, S.; Harnroongroj, T. Effect of active and passive smoking on heavy metals toxic and antioxidant trace elements. *J. Med. Bioeng.* **2016**, *5* (1), 58.
- (28) Pinto, E.; Cruz, M.; Ramos, P.; Santos, A.; Almeida, A. Metals transfer from tobacco to cigarette smoke: Evidences in smokers' lung tissue. *J. Hazard. Mater.* **2017**, *325*, 31–35.
- (29) Yu, Y.-L.; Zhuang, Y.-T.; Song, X.-Y.; Wang, J.-H. Lyophilized carbon nanotubes/graphene oxide modified cigarette filter for the effective removal of cadmium and chromium from mainstream smoke. *Chem. Eng. J.* **2015**, *280*, 58–65.
- (30) Mayer, B. How much nicotine kills a human? Tracing back the generally accepted lethal dose to dubious self-experiments in the nineteenth century. *Arch. Toxicol.* **2014**, *88* (1), 5–7.
- (31) Mishra, A.; Chaturvedi, P.; Datta, S.; Sinukumar, S.; Joshi, P.; Garg, A. Harmful effects of nicotine. *Indian J. Med. Paediatr. Oncol.* **2015**, *36* (1), 24.
- (32) Gao, L.; Cao, Y.; Zhou, S. L.; Zhuang, T. T.; Wang, Y.; Zhu, J. H. Eliminating carcinogenic pollutants in environment: Reducing the tobacco specific nitrosamines level of smoke by zeolite-like calcosilicate. *J. Hazard. Mater.* **2009**, *169* (1–3), 1034–1039.
- (33) Zhou, W.; Xu, Y.; Wang, D.; Zhou, S. Chitosan removes toxic heavy metal ions from cigarette mainstream smoke. *J. Ocean Univ. China* **2013**, *12* (3), 509–514.
- (34) Li, G.; Yu, H.; Xu, L.; Ma, Q.; Chen, C.; Hao, Q.; Qian, Y. General synthesis of carbon nanocages and their adsorption of toxic compounds from cigarette smoke. *Nanoscale* **2011**, *3* (8), 3251–3257.
- (35) Zhou, S.; Ning, M.; Zhang, Y.; He, Q.; Wang, X.; Zhu, D.; Guo, S.; Hong, N.; Hu, Y. Significant removal of harmful compounds in mainstream cigarette smoke using carbon nanotubes mixture prepared by catalytic pyrolysis. *Adsorpt. Sci. Technol.* **2014**, *32* (6), 453–464.
- (36) Chen, Z.; Zhang, L.; Tang, Y.; Jia, Z. Adsorption of nicotine and tar from the mainstream smoke of cigarettes by oxidized carbon nanotubes. *Appl. Surf. Sci.* **2006**, *252* (8), 2933–2937.
- (37) Deng, Q.; Huang, C.; Xie, W.; Zhang, J.; Zhao, Y.; Hong, Z.; Pang, A.; Wei, M. Significant reduction of harmful compounds in tobacco smoke by the use of titanate nanosheets and nanotubes. *Chem. Commun.* **2011**, *47* (21), 6153–6155.
- (38) Deng, Q.; Huang, C.; Zhang, J.; Xie, W.; Xu, H.; Wei, M. Selectively reduction of tobacco specific nitrosamines in cigarette smoke by use of nanostructural titanates. *Nanoscale* **2013**, *5* (12), 5519–5523.
- (39) Armitage, A.; Turner, D. Absorption of nicotine in cigarette and cigar smoke through the oral mucosa. *Nature* **1970**, *226* (5252), 1231.
- (40) Hubetska, T.; Khainakova, O.; Kobylinska, N.; Garcia, J. R. Spherical Mesoporous Carbon Adsorbents for Sorption, Concentration, and Extraction of Nicotine and Other Components of Cigarette Smoke. *Prot. Met. Phys. Chem. Surf.* **2019**, *55* (3), 423–432.
- (41) Sproull, R. C.; Berger, R. M., Smoke filter. US Patent US3353543A, 1967.
- (42) Seligman, R. B.; Carroll, T., Fibrous cigarette filter. US Patent US3101723A, 1963.
- (43) Touey, G. P., Fibrous tobacco smoke filters. US Patent US2928399A, 1959.
- (44) Yoosofian, M.; Pakpour, A.; Etmnan, N. Nanofilter platform based on functionalized carbon nanotubes for adsorption and elimination of Acrolein, a toxicant in cigarette smoke. *Appl. Surf. Sci.* **2018**, *444*, 598–603.

- (45) Yoosefian, M. A high efficient nanostructured filter based on functionalized carbon nanotube to reduce the tobacco-specific nitrosamines, NNK. *Appl. Surf. Sci.* **2018**, *434*, 134–141.
- (46) Wang, Z.; Tu, Q.; Zheng, S.; Urban, J. J.; Li, S.; Mi, B. Understanding the aqueous stability and filtration capability of MoS<sub>2</sub> membranes. *Nano Lett.* **2017**, *17* (12), 7289–7298.
- (47) Liu, H.; Wang, H.; Zhang, X. Facile fabrication of freestanding ultrathin reduced graphene oxide membranes for water purification. *Adv. Mater.* **2015**, *27* (2), 249–254.
- (48) Németh, Z.; Szekeres, G. P.; Schabikowski, M.; Schrantz, K.; Traber, J.; Pronk, W.; Hernádi, K.; Graule, T. Enhanced virus filtration in hybrid membranes with MWCNT nanocomposite. *R. Soc. Open Sci.* **2019**, *6* (1), 181294.
- (49) Yang, Y.; Yang, X.; Liang, L.; Gao, Y.; Cheng, H.; Li, X.; Zou, M.; Ma, R.; Yuan, Q.; Duan, X. Large-area graphene-nanomesh/carbon-nanotube hybrid membranes for ionic and molecular nanofiltration. *Science* **2019**, *364* (6445), 1057–1062.
- (50) Li, H.; Song, Z.; Zhang, X.; Huang, Y.; Li, S.; Mao, Y.; Ploehn, H. J.; Bao, Y.; Yu, M. Ultrathin, molecular-sieving graphene oxide membranes for selective hydrogen separation. *Science* **2013**, *342* (6154), 95–98.
- (51) Srivastava, A.; Srivastava, O.; Talapatra, S.; Vajtai, R.; Ajayan, P. Carbon nanotube filters. *Nat. Mater.* **2004**, *3* (9), 610.
- (52) Bolisetty, S.; Mezzenga, R. Amyloid–carbon hybrid membranes for universal water purification. *Nat. Nanotechnol.* **2016**, *11* (4), 365.
- (53) Pandey, S. K.; Teotia, S.; Srivastava, A. Formation of Large Area Conducting Paper of Carbon Nanotubes for Electrode Applications. *Int. J. Mater. Sci.*, **2017**, *12*, 1.
- (54) Ge, J.; Shi, J.; Chen, L. Gelatin-based carbon microspheres with a foam-like core/solid shell structure. *Carbon* **2009**, *47* (4), 1192–1195.
- (55) Zhao, S.; Wang, C.-Y.; Chen, M.-M.; Sun, J.-H. Mechanism for the preparation of carbon spheres from potato starch treated by NH<sub>4</sub>Cl. *Carbon* **2009**, *47* (1), 331–333.
- (56) Chen, X.; Chen, C.; Chen, Q.; Cheng, F.; Zhang, G.; Chen, Z. Non-destructive purification of multi-walled carbon nanotubes produced by catalyzed CVD. *Mater. Lett.* **2002**, *57* (3), 734–738.
- (57) Bom, D.; Andrews, R.; Jacques, D.; Anthony, J.; Chen, B.; Meier, M. S.; Selegue, J. P. Thermogravimetric analysis of the oxidation of multiwalled carbon nanotubes: evidence for the role of defect sites in carbon nanotube chemistry. *Nano Lett.* **2002**, *2* (6), 615–619.
- (58) Xuan, S.; Hao, L.; Jiang, W.; Gong, X.; Hu, Y.; Chen, Z. A facile method to fabricate carbon-encapsulated Fe<sub>3</sub>O<sub>4</sub> core/shell composites. *Nanotechnology* **2007**, *18* (3), 035602.
- (59) Huang, C.-W.; Chiu, S.-C.; Lin, W.-H.; Li, Y.-Y. Preparation and characterization of porous carbon nanofibers from thermal decomposition of poly (ethylene glycol). *J. Phys. Chem. C* **2008**, *112* (4), 926–931.
- (60) Ju, Z.; Wang, T.; Wang, L.; Xing, Z.; Xu, L.; Qian, Y. A simple pyrolysis route to synthesize leaf-like carbon sheets. *Carbon* **2010**, *48* (12), 3420–3426.
- (61) Branton, P.; Lu, A.-H.; Schüth, F. The effect of carbon pore structure on the adsorption of cigarette smoke vapour phase compounds. *Carbon* **2009**, *47* (4), 1005–1011.
- (62) Fonseca, A.; Viana, M.; Pérez, N.; Alastuey, A.; Querol, X.; Kaminski, H.; Todea, A.; Monz, C.; Asbach, C. Intercomparison of a portable and two stationary mobility particle sizers for nanoscale aerosol measurements. *Aerosol Sci. Technol.* **2016**, *50* (7), 653–668.
- (63) Yi, J.; LeBouff, R. F.; Duling, M. G.; Nurkiewicz, T.; Chen, B. T.; Schwegler-Berry, D.; Virji, M. A.; Stefaniak, A. B. Emission of particulate matter from a desktop three-dimensional (3D) printer. *J. Toxicol. Environ. Health, Part A* **2016**, *79* (11), 453–465.
- (64) Yu, T.; Zhang, X.; Zhong, L.; Cui, Q.; Hu, X.; Li, B.; Wang, Z.; Dai, Y.; Zheng, Y.; Bin, P. The use of a 0.20  $\mu\text{m}$  particulate matter filter decreases cytotoxicity in lung epithelial cells following air-liquid interface exposure to motorcycle exhaust. *Environ. Pollut.* **2017**, *227*, 287–295.
- (65) Clayton, P. M.; Vas, C. A.; Bui, T. T.; Drake, A. F.; McAdam, K. Spectroscopic studies on nicotine and nornicotine in the UV region. *Chirality* **2013**, *25* (5), 288–293.
- (66) Girão, E. C.; Fagan, S. B.; Zanella, I.; Souza Filho, A. G. Nicotine adsorption on single wall carbon nanotubes. *J. Hazard. Mater.* **2010**, *184* (1–3), 678–683.
- (67) Harris, E.; Kay, H. Size distribution of tobacco smoke particles. *Nature* **1959**, *183* (4663), 741–742.
- (68) Keith, C. Particle size studies on tobacco smoke. *Beiträge zur Tabakforschung/Contributions to Tobacco Research* **1982**, *11* (3), 123–131.
- (69) Molaeipour, Y.; Gharehaghaji, A. A.; Bahrami, H. Filtration performance of cigarette filter tip containing electrospun nanofibrous filter. *J. Ind. Text.* **2015**, *45* (2), 187–198.